Journal of Biomedical Optics

SPIEDigitalLibrary.org/jbo

Photoinduced spectral changes of photoluminescent gold nanoclusters

Marija Matulionytė
Raminta Marcinonytė
Ričardas Rotomskis

SPIE

Photoinduced spectral changes of photoluminescent gold nanoclusters

Marija Matulionytė,[a,b] Raminta Marcinonytė,[a] and Ričardas Rotomskis[a,b,*]
[a]National Cancer Institute, Biomedical Physics Laboratory, P. Baublio Street 3b, LT-08406 Vilnius, Lithuania
[b]Vilnius University, Biophotonics Group of Laser Research Centre, Sauletekio Avenue 9, LT-10222 Vilnius, Lithuania

Abstract. Ultrasmall photoluminescent gold nanoclusters (Au NCs), composed of several atoms with sizes up to a few nanometers, have recently stimulated extensive interest. Unique molecule-like behaviors, low toxicity, and facile synthesis make photoluminescent Au NCs a very promising alternative to organic fluorophores and semiconductor quantum dots (QDs) in broad ranges of biomedical applications. However, using gold nanoparticles (Au NPs) for bioimaging might cause their degradation under continuous excitation with UV light, which might result in toxicity. We report spectral changes of photoluminescent 2-(*N*-morpholino) ethanesulfonic acid (MES)-coated (Au-MES) NCs under irradiation with UV/blue light. Photoluminescent water soluble Au-MES NCs with a photoluminescence (PL) band maximum at 476 nm ($\lambda_{ex} = 420$ nm) were synthesized. Under irradiation with 402 nm wavelength light the size of photoluminescent Au-MES NCs decreased ($\lambda_{em} = 430$ nm). Irradiating the sample solution with 330 nm wavelength light, nonluminescent Au NPs were disrupted, and photoluminescent Au NCs ($\lambda_{em} = 476$ nm) were formed. Irradiation with 330 nm wavelength light did not directly affect photoluminescent Au-MES NCs, however, increase in PL intensity indicated the formation of photoluminescent Au NCs from the disrupted nonluminescent Au NPs. This study gives a good insight into the photostability of MES-coated Au NPs under continuous excitation with UV/blue light. [DOI: 10.1117/1.JBO.20.5.051018]

Keywords: photoluminescent gold nanoclusters; spectroscopy; photostability; photoproduct; irradiation; size evaluation; atomic force microscopy; transmission electron microscopy.

Paper 140570SSR received Sep. 3, 2014; accepted for publication Nov. 11, 2014; published online Dec. 17, 2014.

1 Introduction

Gold nanoparticles (Au NPs), typically with sizes of 0.3 to 110 nm, are widely studied due to their remarkable optical, electrical, and chemical properties.[1–4] Conventional Au NPs, bigger than 2 nm, exhibit an extremely high density resulting in collective oscillation of free electrons under excitation with light, also known as surface plasmon resonance.[5–7] The ultrasmall size of photoluminescent gold nanoclusters (Au NCs) comparable to the Fermi wavelength of electrons (~0.7 nm) induces distinctive quantum confinement effects,[8–11] which result in unique molecule-like behaviors due to discrete energy levels. Over the past decade, photoluminescent Au NPs, composed of several atoms to a few nanometers, have been developed and have stimulated extensive interest.[12] Low toxicity and facile synthesis under eco-friendly conditions make photoluminescent Au NCs a very promising alternative to organic fluorophores and semiconductor quantum dots (QDs) in broad ranges of biomedical research and applications. Under certain conditions, UV light is used to initiate synthesis of Au NPs.[13–16] On the other hand, UV photons have high energies and might induce other effects on already synthesized Au NPs, inducing their decomposition. There are very few reports on the photoluminescence stability of Au NCs under irradiation with UV light.[17–20] Some authors have reported photoluminescence instability of dimethylformamide (DMF) protected Au NCs;[17] however, prolonged studies showed that the photostability of DMF-protected Au NCs is higher compared to trypsin stabilized Au NCs.[18] There are also papers showing that the photostability of photoluminescent Au NCs coated with dihydrolipoic acid (DHLA) overcomes the photostability of organic fluorophores, such as fluorescein and rhodamin 6G, but yields to the photostability of hydrophilic polymer-coated CdSe/ZnS QDs.[19] One of the most photostable was ribonuclease-A-encapsulated Au NCs[20] which leads to the conclusion that the photostability of photoluminescent Au NCs varies according to the coating material. Despite the inert nature of gold and the reported stability of Au NPs, using Au NPs for bioimaging might cause their degradation under continuous excitation with UV/blue light,[21] resulting in toxicity. It should be stressed that photostability is the major characteristic of any marker for microscopy, optical imaging, and biopsy. Therefore, the study of photostability and photoluminescence bleaching under continuous excitation with UV/blue light has to be investigated before applying photoluminescent Au NCs for the imaging of biological objects.

In this paper, we present a comprehensive study on the spectroscopic characteristics and photostability of photoluminescent 2-(*N*-morpholino) ethanesulfonic acid (MES)-coated Au NCs under irradiation with near-ultraviolet and visible light.

2 Materials and Methods

2.1 *Chemicals*

2-(N-morpholino) ethanesulfonic acid, (MES) [(>98.0%), Tokyo Chemical Industry, Belgium], sodium hydroxide [NaOH, pellets (>99%), Sigma-Aldrich, Germany] and

*Address all correspondence to: Ričardas Rotomskis, E-mail: Ricardas.Rotomskis@nvi.lt

0091-3286/2015/$25.00 © 2015 SPIE

chloroauric acid [$HAuCl_4 \cdot H_2O$ (99.9%), Sigma-Aldrich, Germany] were used for the synthesis of MES-capped Au NPs.

2.2 *Synthesis of Au-MES NPs*

The Au NPs capped with MES were synthesized according to the modified synthesis protocol of Bao et al.:[22] 5 ml of aqueous MES buffer solution (1 M, pH 6.3, the pH value was achieved using NaOH) was mixed with 1 ml of chloroauric acid solution (0.29 M). Synthesis was performed under vigorous stirring for 21.5 h at the temperature of 37°C.

After the synthesis solution, the Au NPs were centrifuged for 30 min (10,000 rpm or $g = 6.7 \times 10^3$) with a "MiniSpin plus" centrifuge (WTW GmbH, Germany).

The synthesized colloidal solution of MES-coated Au NPs exhibited a deep red color in the daylight and greenish blue photoluminescence under UV light (Fig. 1 inset).

2.3 *Spectrometric Measurements*

Absorption spectra were measured with a Varian Cary Win UV absorption spectrometer (Varian Inc., Australia). Photoluminescence and photoluminescence excitation spectra were measured with a Varian Cary Eclipse fluorescence spectrometer (Varian Inc., Australia) (excitation and emission slits were 5 nm). For all spectrometric measurements, quartz cuvettes of a 1 cm optical path were used (Hellma Optik, Germany).

2.4 *Measurements of Spatial Characteristics*

The size of Au-MES NPs was investigated using atomic force microscope diInnova (Veeco Inc.) and electron transmission microscope FEI TECNAI F20 (FEI) equipped with a field emission electron gun. Atomic force microscopy (AFM) measurements were performed in the tapping mode at 1 Hz with a 9.7 nm step. Samples for AFM measurements were prepared by spreading a drop (40 μl) of colloidal Au-MES NPs solution on a freshly cleaved mica surface using a spin-coating technique (1000 rpm). Transmission electron microscopy (TEM) measurements were performed using an accelerating voltage of 200 kV and bright field images recorded on Orius SC1000B CCD camera (Gatan Inc.). Samples for TEM measurements were prepared by letting a drop (40 μl) of colloidal Au-MES NPs solution dry on a holey carbon film (Mesh grid 400, Agarscientific, UK).

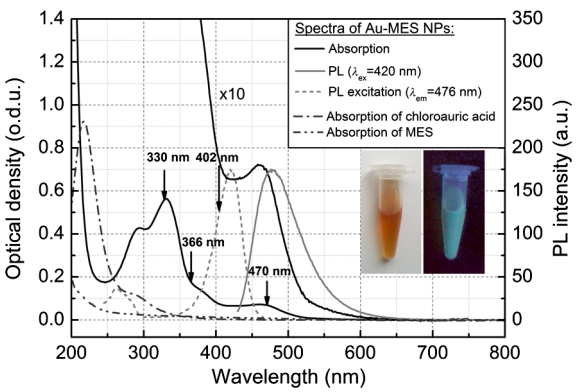

Fig. 1 Absorption, photoluminescence ($\lambda_{ex} = 420$ nm), and PL excitation ($\lambda_{em} = 476$ nm) spectra of Au-MES NPs; absorption spectra of chlorauric acid and MES buffer solution. Arrows represent the wavelengths of irradiation used in photostability measurements. Inset shows images of Au-MES NPs solution in the daylight and under illumination with UV light.

2.5 *Photostability Measurements*

Photostability (photobleaching) measurements of Au NPs were performed by irradiating 2 ml of the sample solution in a 1 cm path length quartz cuvette with an optical fiber coupled xenon (Xe) lamp MAX-302 (A-sashi Tech., Japan) using 402, 330, 366, and 470 nm filters. The collimated beam irradiated 1 cm^2 of the cuvette surface area with a 20 mW light power. The irradiation dose was calculated as the light intensity multiplied by the irradiation time. For all the experiments, a total irradiation dose of ~100 J/cm^2 was accumulated. The PL intensity of Au-MES NPs was normalized according to absorbance at the PL excitation wavelength ($\lambda_{ex} = 405$ nm). Absorption difference spectra were calculated by subtracting the absorption spectrum of Au-MES NPs solution measured before irradiation from the absorption spectrum of Au-MES NPs solution measured after a particular irradiation dose was accumulated.

3 Results

3.1 *Characterization of Au-MES NPs*

Absorption spectrum of synthesized Au-MES NPs (Fig. 1) had a main peak with a maximum at 330 nm, two peaks of lower absorbance at 290 and 475 nm, and one less expressed band at around 390 nm. Components used for the synthesis did not have absorption bands in these spectral regions (Fig. 1). Photoluminescence of Au-MES NPs with a maximum at 476 nm wavelength ($\lambda_{ex} = 420$ nm) (Fig. 1) was detected. The photoluminescence excitation spectrum registered at the photoluminescence maximum ($\lambda_{em} = 476$ nm) (Fig. 1) had a main maximum at 420 nm and another band of lower intensity at around the 260 nm wavelength. The PL excitation spectrum did not coincide with the absorption spectrum of Au-MES NPs.

3.2 *Photostability of Au-MES NPs*

Under irradiation at around the maximum of the photoluminescence excitation band of Au-MES NCs ($\lambda_{irr} = 402$ nm), a slight decrease of absorbance of Au-MES NPs in the spectral region from 250 to 550 nm was detected [Fig. 2(a)] as the accumulated irradiation dose increased. Absorption difference spectra revealed several distinct bleaching absorption bands with maxima at 290, 330, 366, 420, and 470 nm. Bleaching absorption bands at 290, 330, 366, and 470 nm corresponded to the bands in the absorption spectrum of Au-MES NPs. However, no correlation in intensity of the absorption bands and the bleaching bands under irradiation with a 402 nm wavelength light was observed. In addition, the bleaching absorption band at 420 nm was indistinguishable in the absorption spectrum and correlated with the main photoluminescence excitation band of Au-MES NCs. Simultaneously, decrease of intensity of PL band ($\lambda_{ex} = 405$ nm) with a maximum at 476 nm and hypsochromic PL band shift by 47 nm which resulted from the formation of a new PL band with a maximum at 430 nm was observed [Fig. 2(b)]. No PL band shift and only a decrease in the PL intensity at 476 nm was observed when the 420 nm excitation wavelength was used [Fig. 2(c)].

Under irradiation of Au-MES NPs colloidal solution with a 366 nm wavelength light, the most intensive decrease in absorbance was observed at around 330 and 470 nm wavelengths

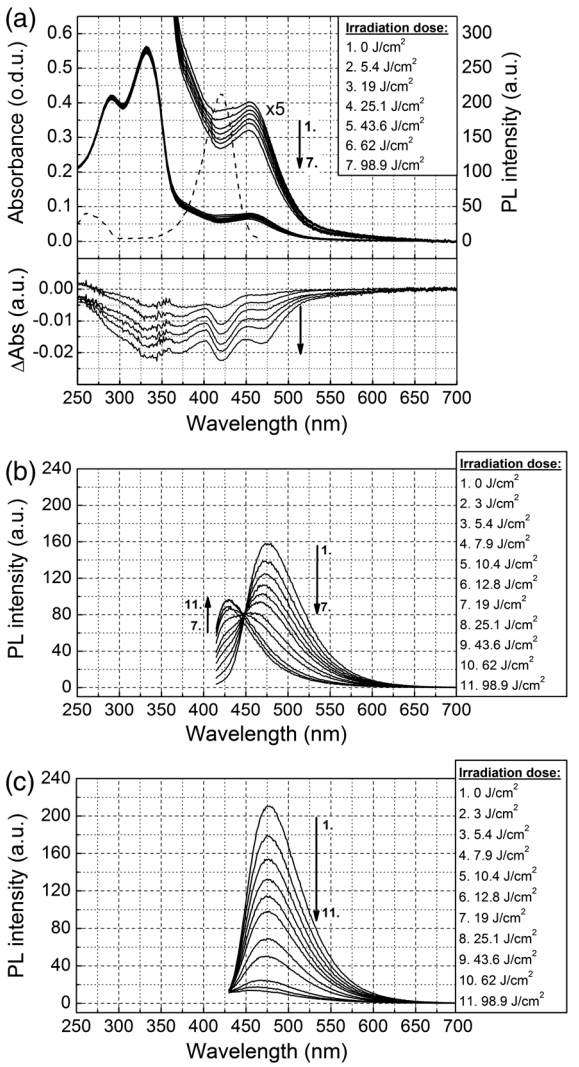

Fig. 2 Spectral changes of Au-MES NPs at $\lambda_{irr} = 402$ nm as accumulated irradiation dose increases. (a) Changes of absorption spectrum (top) and absorption difference spectra (bottom). PL excitation spectrum ($\lambda_{em} = 476$ nm) (dashed curve). (b) Changes of photoluminescence spectrum ($\lambda_{ex} = 405$ nm). (c) Photobleaching of photoluminescence spectrum ($\lambda_{ex} = 420$ nm). Arrows represent the changes in absorbance and PL intensity.

(Fig. 3). Distinct photobleaching bands with maxima at 366 and 420 nm wavelengths were observed in absorption difference spectra. Only the bleaching absorption bands at around 330 and 470 nm corresponded to the absorption bands of Au-MES NPs. PL changes were similar to the ones observed under irradiation with the 402 nm wavelength light (data not shown).

By irradiating Au-MES NPs solution with a near-UV light at 330 nm, the most intensive decrease of the absorbance was detected at around 300 and 470 nm (Fig. 4). At the same time, an increase of the PL ($\lambda_{ex} = 405$ nm) intensity was observed (Fig. 4 inset), although the peak position remained intact. The bleaching band at 300 nm in the absorption difference spectra did not coincide with the one at 330 nm which was observed under irradiation at 366 nm (Fig. 3) indicating that each irradiation wavelength ($\lambda_{irr} = 366$; 330 nm) affected a different fraction of the nonluminescent gold NPs.

When irradiating a colloidal solution of Au-MES NPs with a 470 nm wavelength light, no changes in absorption and PL

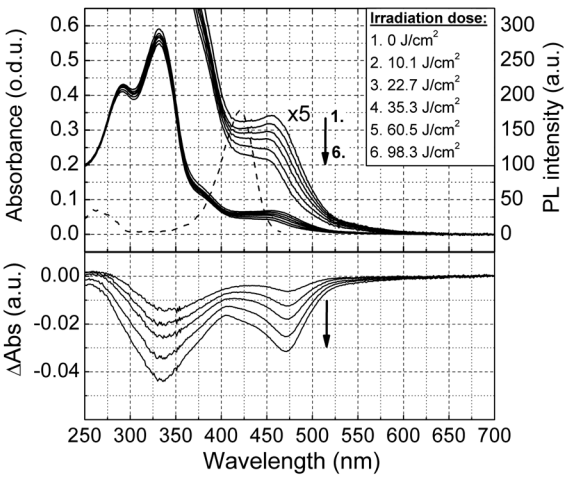

Fig. 3 Changes of absorption spectrum (top) and absorption difference spectra (bottom) of Au-MES NPs at $\lambda_{irr} = 366$ nm as accumulated irradiation dose increases. Arrow represents the changes in absorbance.

spectra were observed even when the maximum irradiation dose of ~100 J/cm^2 was accumulated (data not shown).

4 Discussion

Metal NPs of a size on the same order as the electron Fermi wavelength (~0.5 nm for silver and gold)[23–25] often exhibit strong single electron excitations and emit photoluminescence.[1] Synthesized according to the modified synthesis protocol of Bao et al.[22] colloidal MES-coated Au NPs exhibited a deep red color in the daylight and greenish blue photoluminescence under near-UV excitation (Fig. 1 inset). The absorption spectrum of the synthesized colloidal solution did not coincide with the PL excitation spectrum ($\lambda_{em} = 476$ nm) indicating that there are not only photoluminescent Au NCs but also some nonluminescent substance in the synthesized solution. The PL excitation spectrum had a main maximum at 420 nm and another band of lower intensity at around 260 nm. Absorption bands at 290, 330, 366, and 470 nm correspond to absorption of the nonluminescent Au-MES NPs. Nevertheless, there is no absorption in the

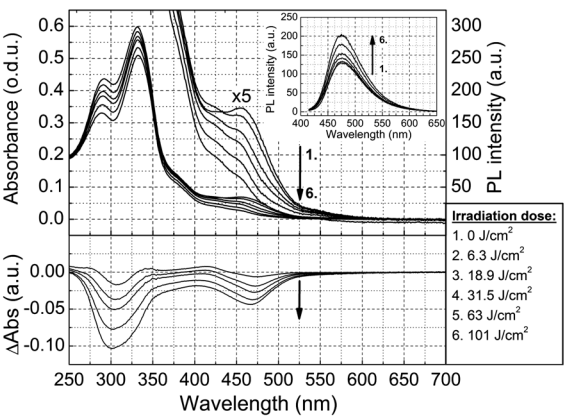

Fig. 4 Changes of absorption spectrum (top) and absorption difference spectra (bottom) of Au-MES NPs at $\lambda_{irr} = 330$ nm as accumulated irradiation dose increases. PL excitation spectrum ($\lambda_{em} = 476$ nm) (dashed curve). Inset—changes of PL spectrum ($\lambda_{ex} = 405$ nm). Arrows represent the changes in absorbance and PL intensity.

spectral region above 510 nm that would indicate the existence of Au NPs exhibiting localized surface plasmon resonance (LSPR).[5–7] According to the literature, the NPs that are bigger than 4 nm in diameter exhibit LSPR.[5,6] In contradiction to that, up to 10 nm and up to 6 nm diameter Au NPs were detected using atomic force microscopy and TEM, respectively (Fig. 5). The discrepancy between those results could be due to differences of the two techniques, as TEM gives us only the size of the core of the Au-MES NPs and atomic force microscopy gives the size of the NPs, which is several nanometers bigger than the core itself due to the MES coating. From our measurements, we can clearly state that several distinct types of Au-MES NPs could be distinguished: very small (<1 nm) photoluminescent Au NCs (observed only with AFM), and other Au NPs below 10 nm in diameter.

Four different wavelengths were selected for irradiation of Au-MES NPs. Irradiation at 402 nm was preferentially absorbed by photoluminescent Au-MES NCs as the irradiation wavelength is in the range of their PL excitation band. Absorption by other nonluminescent gold NPs at 402 nm was minimal due to the minimum absorbance of the sample at this wavelength (Fig. 1). The appearance of the bleaching band at 420 nm in the absorption difference spectrum [Fig. 2(a)] that coincides with the maximum of the PL excitation spectrum and the simultaneous decrease of PL intensity at 476 nm [Figs. 2(b) and 2(c)] revealed that photoluminescent Au-MES NCs were irradiation-disrupted. However, a hypsochromic shift of the PL band position and the appearance of the new PL band at 430 nm suggested that under irradiation with 402 nm wavelength light a new type of photoluminescent NCs with a PL peak at the 430 nm wavelength were formed [Fig. 2(b)].

Following a free electron gas (Jellium) model,[23,26] a number of gold atoms N in small Au NCs can be calculated from the PL band position with a simple equation

$$N = (e\lambda_{\max} E_F/hc)^3, \quad (1)$$

where e is a number equal to the electron charge, $\lambda_{\max}$ is a wavelength at the emission band maximum, E_F is the Fermi energy of bulk gold (5.53 eV), h is the Planck constant, and c is the speed of light. According to the calculations, the NPs that exhibit a PL shift to a shorter wavelength region are smaller and consist of fewer atoms.[8–11] So, the blue shift of PL band of Au-MES NPs under irradiation at 402 nm could be explained by the formation of Au NCs consisting of fewer atoms. According to the calculations, Au NPs that exhibit photoluminescence at 476 nm wavelength consist of ~9 gold atoms. As the PL band maximum has shifted to 430 nm wavelength, the number of gold atoms must have decreased to 7.

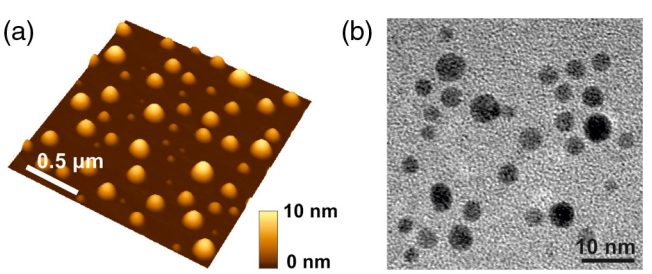

Fig. 5 (a) Topography of Au-MES NPs on a mica surface (AFM image) and (b) STEM image of Au-MES NPs on a carbon film.

Irradiating Au-MES NCs with a 402 nm wavelength light, the discrete hypsochromic shift of the PL band revealed the formation of a photoproduct—smaller photoluminescent Au NCs of particular size. However, so far there are no other results published claiming that light would reduce the size of photoluminescent Au NCs, though a decrease of the PL intensity has been reported for DMF-, trypsin-, and DHLA-stabilized Au NCs under irradiation with near-UV light.[17–19] In contrast, irradiation of photoluminescent semiconductor QDs with UV/Vis light is well known to affect PL quantum yield[27–29] and induce a continuous hypsochromic[27,28] or bathochromic[29] shift of the PL band indicating photoetching and aggregation of QDs, respectively. However, a discrete spectral shift of Au-MES NCs suggesting a molecule-like behavior[30] complicates comparison of photoluminescent Au NCs with semiconductor QDs that undergo a continuous shift of the PL band under irradiation with UV/Vis light.[27–29]

Absorption difference spectra revealed that under irradiation with 402 nm wavelength light, absorbance decreased not only at the 420 nm wavelength, but a slight photobleaching of the absorption was detected in all spectral range from 250 to 550 nm [Fig. 2(a)] showing that bigger nonluminescent NPs were also affected by irradiation. When irradiating the sample solution at $\lambda_{irr} = 330$ nm at the main absorption peak not related to photoluminescent Au NCs, a decrease of absorbance at around 300 nm and 470 nm wavelengths was observed (Fig. 4) indicating the decomposition of nonluminescent Au-MES NPs. However, the shape of absorption difference spectrum did not coincide with the shape of the absorption spectrum of Au-MES NPs (Fig. 6) showing that under irradiation at 330 nm, only part of the nonluminescent Au-MES NPs were disrupted. The most sensitive to the irradiation at 330 nm were Au-MES NPs with a strong absorption at 300 nm (I type). The new bleaching absorption band with a maximum at 330 nm appeared, irradiating the sample solution at a wavelength slightly shifted to the red spectral range ($\lambda_{irr} = 366$ nm) (Fig. 3). This absorption band could be assigned to another type (II type) of the nonluminescent Au-MES NPs which have a main absorption band at 330 nm wavelength. Discrepant changes in absorption difference spectra under irradiation at different wavelengths suggests that the absorption spectrum of Au-MES NPs is a superposition of the absorption of photoluminescent Au-MES NCs and of the minimum two different fractions of nonluminescent Au-MES NPs.

An increase in PL intensity at 476 nm that occurred simultaneously with the decrease of absorbance under irradiation at 330 nm (Fig. 4) must have occurred due to the disruption of bigger nonluminescent Au-MES NPs and formation of photoluminescent NCs from their remains as the PL intensity in

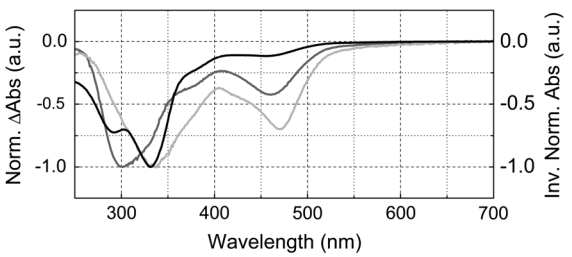

Fig. 6 Inverted normalized absorption spectrum of Au-MES NPs (black) and normalized absorption difference spectra of Au-MES NPs under irradiation at 330 nm (dark gray) and at 366 nm (light gray).

the PL excitation spectrum at 330 nm is negligible and irradiation did not directly affect photoluminescent Au-MES NCs.

The low-power irradiation (20 mW) used in our experiments could not induce high energy related processes such as ablation of solid materials producing NCs that can be achieved using high-energy pulsed-lasers.[31–34] However, it has been shown that low-power irradiation with UV light can induce formation of Au NPs from chlorauric acid.[14] Irradiation of Au NPs (17 to 23 nm in diameter) with low-power UV light can also induce generation of one or a few reactive oxygen species (ROS) such as hydroxyl radicals (•OH), singlet oxygen ($^1O_2$), superoxide radicals ($O_2^{\bullet -}$).[35,36] Despite the fact that Zhang et al. have shown that under UV exposure of Au NPs (17 to 23 nm in size) no gold ions were detected,[36] upon irradiation with 402 nm (as with 366 nm) wavelength light, the size of the photoluminescent Au NCs (<1 nm in diameter) decreased, and irradiation at 330 nm disrupted the nonluminescent NPs (<10 nm in diameter). The greater effects on Au-MES NPs such as disruption and a decrease in size could have appeared due to increased ROS generation since under irradiation with x-rays, smaller Au NPs generate more ROS than bigger NPs due to increased surface area to volume ratio.[35]

5 Conclusions

In summary, the synthesized photoluminescent Au-MES NCs are not photostable under irradiation with UV/blue light. Upon irradiation at 402 nm, the photoluminescent Au-MES NCs (<1 nm in diameter) ($\lambda_{em} = 476$ nm) transform into a new type of photoluminescent NCs with an emission band maximum at $\lambda_{em} = 430$ nm. The calculations show that the size of the photoluminescent NCs decreases from ~9 to ~7 gold atoms. Moreover, nonluminescent gold NPs are also nonphotostable: disrupting the I type of nonluminescent gold NPs under irradiation at 330 nm, the photoluminescent Au NCs with an emission band maximum at $\lambda_{em} = 476$ nm were formed. However, irradiation at 366 nm to the absorption of the II type of nonluminescent Au-MES NPs resulted only in the disruption of photoluminescent and nonluminescent gold NPs. The spectral changes of Au-MES NPs upon irradiation with UV/blue light could be related to the generation of ROS. Further research is required to fully investigate the photoinduced processes in NPs under low-power irradiation.

Acknowledgments

This work was financially supported by the Joint Lithuanian-Latvian-Chinese (Taiwanese) Tripartite Cooperation Programme, Grant No. TAP-LLT-13-016, by the World Federation of Scientists giving National one-year scholarship to M. Matulionytė, by the project "Promotion of Students' Scientific Activities" (VP1-3.1-ŠMM-01-V-02-003) funded by the Republic of Lithuania and European Social Fund giving scholarship to R. Marcinonytė.

References

1. S. F. Lai et al., "Very small photoluminescent gold nanoparticles for multimodality biomedical imaging," *Biotechnol. Adv.* **31**, 362–368 (2013).
2. V. K. A. Sreenivasan, A. V. Zvyagin, and E. M. Goldys, "Luminescent nanoparticles and their applications in the life sciences," *J. Phys. Condens. Matter* **25**, 194101 (2013).
3. Y. Huang et al., "Biomedical nanomaterials for imaging-guided cancer therapy," *Nanoscale* **4**(20), 6135–6149 (2012).
4. A. J. Mieszawska et al., "Multifunctional gold nanoparticles for diagnosis and therapy of disease," *Mol. Pharm.* **10**(3), 831–847 (2013).
5. V. Amendola and M. Meneghetti, "Size evaluation of gold nanoparticles by UV-Vis spectroscopy," *J. Phys. Chem. C* **113**(11), 4277–4285 (2009).
6. W. Haiss et al., "Determination of size and concentration of gold nanoparticles from UV–Vis spectra," *Anal. Chem.* **79**(11), 4215–4221 (2007).
7. P. N. Njoki et al., "Size correlation of optical and spectroscopic properties for gold nanoparticles," *J. Phys. Chem. C* **111**(40), 14664–14669 (2007).
8. X. Yuan et al., "Luminescent noble metal nanoclusters as an emerging optical probe for sensor development," *Chem. Asian J.* **8**(5), 858–871 (2013).
9. S. Palmal and Nikhil R. Jana, "Gold nanoclusters with enhanced tunable fluorescence as bioimaging probes," *Wiley Interdiscip. Rev. Nanomed. Nanobiotechnol.* **6**(1), 102–110 (2014).
10. C. Zhou et al., "Luminescent gold nanoparticles: a new class of nanoprobes for biomedical imaging," *Exp. Biol. Med. (Maywood)* **238**(11), 1199–1209 (2013).
11. L. Zhang and E. Wang, "Metal nanoclusters: new fluorescent probes for sensors and bioimaging," *Nano Today* **9**, 132–157 (2014).
12. J. Zheng, C. Zhang, and R. M. Dickson, "Highly fluorescent water soluble size tunable gold quantum dots," *Phys. Rev. Lett.* **93**(7), 077402 (2004).
13. L. Huang et al., "Synthesis size control and fluorescence studies of gold nanoparticles in carboxymethylated chitosan aqueous solutions," *J. Colloid Interface Sci.* **316**, 398–404 (2007).
14. W. Hao et al., "Time evolution of gold nanoparticles in HPC solution after UV irradiation," *Mater. Lett.* **62**, 3106–3109 (2008).
15. M. M. Chili, V. S. R. R. Pullabhotla, and N. Revaprasadu, "Synthesis of PVP capped gold nanoparticles by the UV-irradiation technique," *Mater. Lett.* **65**, 2884–2847 (2011).
16. G. N. Abdelrasoul et al., "Photochemical synthesis: effect of UV irradiation on gold nanorods morphology," *J. Photochem. Photobiol. A* **275**, 7–11 (2014).
17. H. Kawasaki et al., "Stability of the DMF-protected Au nanoclusters: photochemical dispersion and thermal properties," *Langmuir* **26**(8), 5926–5933 (2010).
18. H. Kawasaki et al., "Trypsin-stabilized fluorescent gold nanocluster for sensitive and selective Hg^{2+} detection," *Anal. Sci.* **27**, 591–596 (2011).
19. C. A. J. Lin et al., "Synthesis, characterization, and bioconjugation of fluorescent gold nanoclusters toward biomedical labeling application," *ACS Nano* **3**(2), 395–401 (2009).
20. Y. Kong et al., "Near-infrared fluorescent ribonuclease-A-encapsulated gold nanoclusters: preparation, characterization, cancer targeting and imaging," *Nanoscale* **5**, 1009–1017 (2013).
21. R. Marcinonytė, M. Matulionytė, and R. Rotomskis, "Stability and photostability of MES capped gold nanoparticles," in *Proc. of 10th Int. Conf. and Workshop "Medical Physics in the Baltic States,"* Vol. 10, pp. 62–66, Kaunas, Lithuania, Kaunas University Technology Press (2012).
22. Y. Bao et al., "Formation and stabilization of fluorescent gold nanoclusters using small molecules," *J. Phys. Chem. C* **114**(38), 15879–15882 (2010).
23. H. Haberland, "Clusters of atoms and molecules: theory experiment, and clusters of atoms," in *Springer Series in Chemical Physics*, Vol. 56, pp. 422, Springer-Verlag, Berlin, Germany (1994).
24. R. Kubo, "Electronic properties of metallic fine particles," *J. Phys. Soc. Jpn.* **17**, 975–986 (1962).
25. T. G. Schaaff et al., "Isolation and selected properties of a 10.4 kDa gold: glutathione cluster compound," *J. Phys. Chem. B* **102**(52), 10643–10646 (1998).
26. U. Kreibig and M. Vollmer, "Optical properties of metal clusters," in *Springer Series in Materials Science*, Vol. 25, pp. 535, Springer-Verlag, Berlin, Germany (1995).
27. A. Ramanavičius et al., "Stabilization of (CdSe)ZnS quantum dots with polypyrrole formed by UV/VIS irradiation initiated polymerization," *J. Nanosci. Nanotechnol.* **9**, 1909–1915 (2009).

28. E. A. Christensen, P. Kulatunga, and B. C. Lagerholm, "A single molecule investigation of the photostability of QDs," *PLoS One* **7**(8), e44355 (2012).
29. F. Aldeek et al., "Enhanced photostability from CdSe(S)/ZnO core/shell quantum and their use in biolabeling," *Eur. J. Inorg. Chem.* **2011**, 794–801 (2011).
30. R. Rotomskis, G. Streckytė, and S. Bagdonas, "Phototransformation of sensitizers 1. Significance of the nature of the sensitizers in the photobleaching process and photoproduct formation in aqueous solution," *J. Photochem. Photobiol. B* **39**, 167–171 (1997).
31. A. Schwenke et al., "Non-agglomerated gold-PMMA nanocomposites by in situ-stabilized laser ablation in liquid monomer for optical applications," *Appl. Phys. A* **111**, 451–457 (2013).
32. R. Kubiliūtė et al., "Ultra-pure, water-dispersed Au nanoparticles produced by femtosecond laser ablation and fragmentation," *Int. J. Nanomed.* **8**, 2601–2611 (2013).
33. A. I. Kuznetsov et al., "Laser induced jet formation and droplet ejection from thin metal films," *Appl. Phys. A* **106**, 479–487 (2012).
34. M. Maciulevičius et al., "Pulsed-laser generation of gold nanoparticles with on-line surface plasmon resonance detection," *Appl. Phys. A* **111**, 289–295 (2013).
35. M. Misawa and J. Takahashi, "Generation of reactive oxygen species induced by gold nanoparticles under x-ray and UV irradiations," *Nanomed. Nanotechnol. Biol. Med.* **7**, 604–614 (2011).
36. W. Zhang et al., "Photogeneration of reactive oxygen species on uncoated silver gold nickel and silicon nanoparticles and their antibacterial effects," *Langmuir* **29**, 4647–4651 (2013).

Marija Matulionytė received her BSc degree in applied physics and her MSc in biophysics from the Faculty of Physics, Vilnius University, in 2010 and 2012, respectively. She is currently a PhD student in physics at Vilnius University (Lithuania) and a junior research scientist at the Biomedical Physics Laboratory, National Cancer Institute, Lithuania. Her research interests include UV/Vis spectroscopy, photostability and structural characterization of nanoparticles and biologically active molecules along with *in vitro* imaging using confocal fluorescence microscopy.

Raminta Marcinonytė received her BSc degree in molecular biology from the Faculty of Natural Sciences, Vilnius University, in 2013. She is currently an MSc student in medical biology at the Faculty of Medicine, Vilnius University. Her research interests include UV/Vis spectroscopy and photostability of nanoparticles and biologically active molecules, and *in vitro* imaging using confocal fluorescence microscopy.

Ričardas Rotomskis is a head of the Biomedical Physics Laboratory at the National Cancer Institute and a professor at the Department of Quantum Electronics, Vilnius University. He received an MSc degree in solid state physics, Vilnius University, Vilnius (Lithuania), a PhD degree in biophysics, M.V. Lomonosov State University, Moscow (Russia), and did postdoctoral work at Leiden University, Leiden (The Netherlands). His research interests include biophotonics, nanophotonics, spectroscopy, primary photophysical and photochemical processes, and photostability of biologically active molecules and nanoparticles (*in vivo* and *in vitro*).